Molecular Orbital Studies of Gas-Phase Interactions between Complex Molecules

Roger Gaudreault,[†,§] M. A. Whitehead,*[,†] and Theo G. M. van de Ven[†,‡]

Department of Chemistry, McGill University, 801 Sherbrooke St. W, Montreal, QC, Canada H3A 2K6, Pulp & Paper Research Centre, McGill University, 3420 University St., Montreal, QC, Canada H3A 2A7, and Cascades Inc., Recherche et Développement, 471 Marie-Victorin boul., Kingsey Falls, QC, Canada J0A 1B0

Received: January 24, 2005

Describing interactions among large molecules theoretically is a challenging task. As an example, we investigated gas-phase interactions between a linear nonionic oligomer and various model compounds (cofactors), which have been reported to associate experimentally, using PM3 semiempirical molecular orbital theory. As oligomer, we studied the hexamer of poly(ethylene oxide) (PEO), and as cofactors, we studied corilagin and related compounds containing phenolic groups (R−OH). These systems are of interest because they are models for PEO/cofactor flocculation systems, used in industrial applications. The PM3 delocalized molecular orbitals (DLMO) describe the bonding between $(PEO)_6$ and cofactors, and some of them cover the complete complex. The DLMOs which cover the traditionally considered hydrogen bonds R−OH···O or R−CH···O show a distinct "pinch", a decrease of the electron density, between the H···O atoms. Calculations of Gibbs free energy, entropy, and enthalpy show that the PEO/cofactor complexes do not form at room temperature, because the loss of entropy exceeds the increase in enthalpy. The change in enthalpy is linearly related to the change in entropy for the different complexes. Even though bond lengths, bond angles, DLMOs, and electron densities for the PEO/cofactor complexes are consistent with the definition of hydrogen bonds, the number of intermolecular R−OH···O and R−CH···O bonds does not correlate with the enthalpy of association, indicating that the bonding mechanism for these systems is the sum of many small contributions of many delocalized orbitals.

Introduction

The flocculation efficiency of poly(ethylene oxide) (PEO) is enhanced by various compounds, known as cofactors, which are believed to associate with PEO.[1−7] The driving force of this association has been attributed to hydrogen bonding between the ether oxygen in PEO and the phenolic hydroxyl groups of the cofactors.

Molecular mechanics,[8] in which the hydrogen bond is built-in, showed that the OH groups of the phenolic rings of the cofactor PFR (phenol−formaldehyde resin) form hydrogen bonds with alternate PEO oxygens 7 Å apart, while the cofactor isotactic PVPh (poly(vinyl phenol)) oligomers[9] gave hydrogen bonds on every fourth or fifth PEO oxygen and the R−OH···O distances were <2.37 Å, with an angle of 130−180°. Hydrogen bonding in a water-insoluble cofactor PVPh/PEO complex was deduced by Zhang et al.,[10] from ^{13}C solid-state NMR. The water-soluble ionic cofactor PVPh-*co*-KSS (poly(vinyl phenol-*co*-potassium styrene sulfonate))/PEO complex gave 1H NMR results that did not exclude hydrogen bonding when the distance between the PEO and the aromatic protons of PVPh-*co*-KSS was less than 5 Å,[11] but opened the discussion that other interactions were possible; indeed, the PEO/cofactor complex forms at pH 12, where the OH groups dissociate. Cong et al.[11] found that the number of ether oxygens per aromatic ring in the complex depended on the molar ratio of PVPh-*co*-KSS/PEO and temperature. At 303 K and a PVPh-*co*-KSS/PEO molar ratio of 0.2, for every phenol moiety there were 4.9 polyether repeat units within 5 Å of an aromatic ring.

Goto et al.[12] studied the flocculation of four colloidal suspensions, precipitated calcium carbonate (PCC), clay, TiO_2, and polystyrene latex, using a combination of polymeric flocculants, PEO, and poly(acrylamide-*co*-PEG) comb copolymer, and cofactors of various structures and charges. They speculated that the surface charge and the density of the phenolic hydroxyl groups in the cofactor are important for flocculating colloids.

More recently, Lu et al.[13] found that water-soluble polypeptides with high tyrosine contents, i.e., phenolic moieties, form complexes with high molecular weight PEO in 1 mM $CaCl_2$. PEO/peptide complexes can be good flocculants; however, the flocculation efficiency is sensitive to the polypeptide structure. PEO/polypeptide complexes are necessary, but not sufficient, for flocculation. Poly(glutamic acid/tyrosine) (1:1) at molecular weight 36.1 kDa caused the flocculation of PCC pretreated with dextran sulfate (PCC + DS) upon the addition of PEO, whereas $(glutamic\ acid/tyrosine)_4$ of molecular weight 1.1 kDa did not; therefore, the molecular weight is important.[13]

Malardier-Jugroot et al.[14] showed that the PM3[15,16] semiempirical molecular orbital theory is reliable for conformational analysis of hydrogen-bonded molecules. Rakotondradany et al.[17] showed that experimental results of self-assembled azodibenzoic acid linear tapes and cyclic tetramers, formed through hydrogen bonds, corroborated the PM3 predictions.

In this work, different conformers of TGG (1,3,6-tri-*O*-galloyl-*β*-D-glucose) and corilagin (*β*-1-*O*-galloyl-3,6-(*R*)-hexahydroxydiphenoyl-D-glucose) were used as model cofactors[18] (Figure 1). They contain phenolic groups, characteristic

* To whom correspondence should be addressed. E-mail: tony.whitehead@mcgill.ca.
† Department of Chemistry, McGill University.
‡ Pulp & Paper Research Centre, McGill University.
§ Cascades Inc.

10.1021/jp050418p CCC: $33.50
Published on Web 02/22/2006

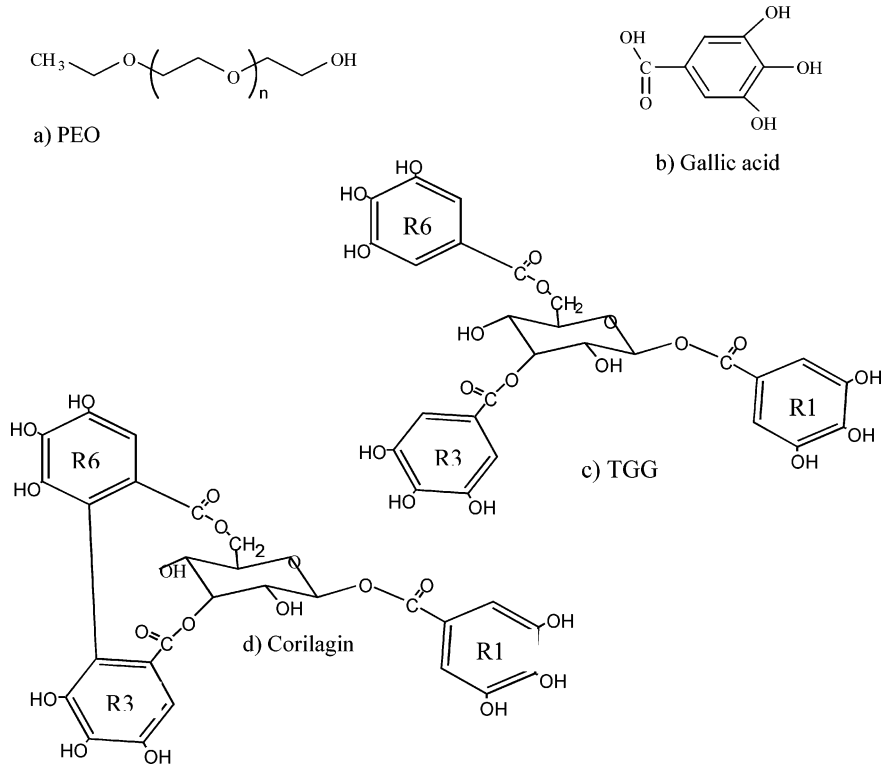

Figure 1. Molecular structures of (a) PEO, (b) gallic acid, (c) TGG, and (d) corilagin. (R1, R3, and R6 designate rings 1, 3, and 6, respectively.)[18]

of real polymeric phenolic cofactors. TGG consists of a sugar ring esterified three times by gallic acid. In TGG, there is no bond between the galloyl rings, giving a flexible structure, which parallels the polymeric phenolic resins used in papermaking. Corilagin[19] is bonded between two galloyl rings, which gives a more rigid structure for comparison. The bond length, bond angle, heat of formation (H_f), Gibbs free energy (G), entropy (S), electron density (ρ), and molecular orbital wave functions of the complexes PEO/gallic acid, PEO/TGG, and PEO/corilagin are discussed. In this work, the PEO/gallic acid complex is assumed to be a hydrogen-bonded reference complex.

Theoretical Methods

The Programs. Theoretical calculations used *Gaussian GW03*[20] revision B.02 and *GaussViewW* version 3.07. PM3[15,16] semiempirical calculations used a convergence limit of 0.005, without configuration interaction. In PEO, gallic acid, TGG, and corilagin, the total charge was zero with no net spin (multiplicity = 1) to start the calculations. Energy minimization used the conjugate gradient Polak Ribiere method, terminated when the root-mean-square (rms) was less than 0.005 kcal mol^{-1} Å^{-1}. The PEO hexamer was built using Cerius^2_3.5/Polymer Builder/Homopolymer[21] using the isotacticity, head-to-tail monomer orientation and torsion angles of 180°, followed by Mopac/PM3[15,16] geometry optimization. Theoretical results were obtained at 0 and 298.15 K using frequency analysis and then scaled by 0.9761 to give theoretical results, which are believed to be closer to experiment.[22] More details about the theories and programs are given in ref 23.

The Conformers. The methods to build the conformers have been described before.[18] The conformers[18] were reoptimized using *Gaussian GW03* revision B.02.[20] Table 1 shows the differences in heats of formation at 0 K using Mopac/PM3 and *Gaussian GW03*/PM3. Conformers are indicated by the conformation of their sugar ring, except for TGG semi-tripod and tripod. All the conformers have lower energies using GW03 than in Mopac,[18] which reflects the more efficient minimization procedure in GW03.[20]

TABLE 1: Heats of Formation of the Conformers of the Cofactors

cofactor	conformer	$H_{f,0\,K}$ (kcal mol^{-1}) PM3/Mopac[18]	$H_{f,0\,K}$ (kcal mol^{-1}) PM3/GW03
TGG	chair	−665.52	−666.66
TGG	semi-tripod	−667.35	−668.48
TGG	tripod	−669.12	−670.42
corilagin[a]	boat	−645.61	−650.24
corilagin[a]	skew-boat	−629.09	−652.23
corilagin[a]	chair	−623.57	−637.57
R1R3[b]	skew-boat	−598.96	−644.13
R1R6[b]	skew-boat	−626.66	−657.52

[a] Corilagin has a covalent bond between R3 and R6. [b] Covalent bond between R1 and R3 or R1 and R6.

In corilagin, the boat and skew-boat conformers have different energies in the two calculations; the GW03 is obviously more efficient in minimizing the energy of more rigid structures. This is supported by the fact that the boat and skew-boat corilagin conformers, which are quite rigid, were energetically quite different in Mopac, −645.61 and −629.09 kcal mol^{-1},[18] and are energetically alike in GW03, −650.24 and −652.23 kcal mol^{-1}. The slightly more stable skew-boat corilagin conformer (−652.23 kcal mol^{-1}) predicted by GW03 is supported by the experimental interpretation of Jochims et al.[24] and Yoshida and Okuda.[25] The reversed Mopac stabilities, −629.09 and −645.61, disagree with their experimental interpretation.[24,25] Interestingly, R1R3 and R1R6, two theoretically conceived structures, generate one structure, R1R6, which is more stable than any of the other corilagin structures, formed from TGG; because it has the same open structure, whereas TGG/R1R3 and corilagin are more compact (Figure 2).

The Complexes. Williams et al.[26] mentioned that, when solvent interactions are ignored and then two molecules A and B associate to form a complex, A and B rearrange their structures to give a more stable complex. Recently, Malardier-

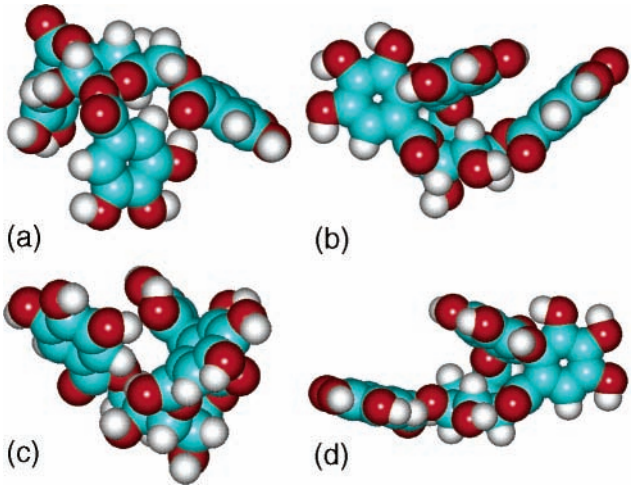

Figure 2. Molecular structures (overlapping spheres model) of (a) TGG, (b) corilagin boat, (c) R1R3, and (d) R1R6.

Jugroot et al.[27,28] showed that the properties of the solutes and their ability or inability to denature proteins can be explained without including the solvent effect.

The present gas-phase calculations show that PEO has two distinct structures: one crystalline[29] with the ether oxygen inside the helical molecule (Figure 3 left) and a more stable gas-phase structure with the ether oxygen outside the helix (Figure 3, right).

The PM3 optimized PEO structures capable of forming complexes with the various cofactors had intermediate structures, A_{opt}. The various cofactors similarly gave B_{opt}, characteristic of the cofactor structures. Equation 1 describes the formation of PEO/cofactor complexes. Initially, A_{opt} and B_{opt} are brought together, changing their conformations to fit into each other; A'_{opt} and B'_{opt} subsequently reoptimized as a complex to give $(A'B'_{opt})$, the most stable complex structure possible.

$$A_{opt} + B_{opt} \rightleftharpoons A'_{opt} + B'_{opt} \rightleftharpoons (A'B'_{opt}) \qquad (1)$$

The hexamer of PEO and the cofactor, either TGG or corilagin, were brought sufficiently close, so that the PEO fits within the cavity of the cofactor. In this conformation, the distance between an ether oxygen of the PEO and a hydroxyl phenolic proton approaches 1.8 Å, the value of a typical hydrogen bond.[30] After a first geometrical optimization, the conformation of the PEO, a very flexible molecule, was changed to increase the number of hydrogen bonds and to maximize the ability of PEO and cofactor to assemble, by docking, until the energetically ($H_{f,0\,K}$) most stable complex was obtained. This method of manipulation was repeated, in some instances up to 26 times, until the enthalpy of association was fully minimized and the PEO/cofactor complex was in a global minimum. This approach was to reflect the current idea that the driving mechanism of complexation between PEO and cofactor is hydrogen bonding between the phenolic hydroxyl group of the cofactor and the PEO ether oxygen.

To find the most stable complex, it was necessary to consider the asymmetrical structure of the cofactors. Consequently, the PEO hexamer was placed at different positions around the cofactor to give structures interacting at the top, bottom, side, and inside the cavity to give the global minimum PEO/cofactor structures shown in Figure 4.

The heats of formation ($H_{f,0\,K}$) of all molecules and complexes were initially calculated at 0 K, giving the enthalpy of association as

$$\Delta H^{(A'B')_{opt}}_{0\,K} = H^{(A'B')_{opt}}_{f,0\,K} - \sum (H^{A_{opt}}_{f,0\,K} + H^{B_{opt}}_{f,0\,K}) \qquad (2)$$

However, it was decided to calculate the enthalpy of association at 298.15 K ($\Delta H^{(A'B')_{opt}}_{298\,K}$), more characteristic of conditions for which PEO/cofactors are used. Consequently, the terms for entropy ($T\Delta S^{(A'B')_{opt}}_{298\,K}$) now come into play, together with the Gibbs free energy ($\Delta G^{(A'B')_{opt}}_{298\,K}$). The values at 298.15 K were calculated from a frequency analysis;[31] to bring the results closer to experiment, the recommended scaling factor of 0.9761[22] was applied to the results obtained at 298.15 K.

Although the interactions between PEO and the model cofactors give weakly bonded complexes, as described by eq 1, it must be remembered that A_{opt} and B_{opt} reconform to give A'_{opt} and B'_{opt}. For simplicity, the subscript opt and primes used as superscript will be omitted in reporting results. Delocalized molecular orbitals (DLMO) and the change in enthalpy as a function of the change in entropy at 298.15 K are used to study the interactions of the complexes.

Results and Discussion

To analyze the complexation, it is necessary to study first PEO and corilagin in isolation, followed by the interactions among them. At first, PEO is considered.

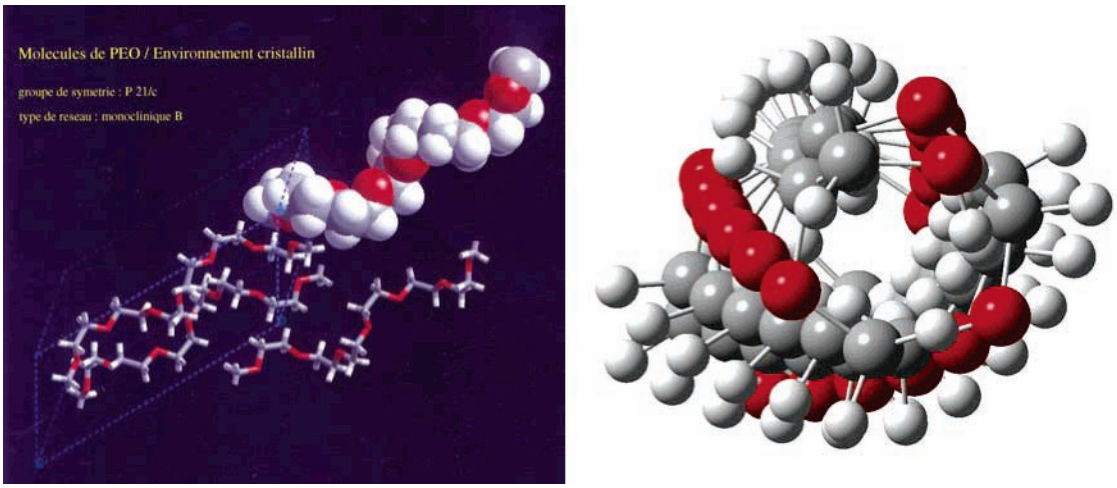

Figure 3. Molecular structure of poly(ethylene oxide) (PEO): crystalline (left); a periodic box is shown together with repeat units, one of which is in the overlapping spheres model representation; and the more stable gas-phase structure (right) obtained by performing a complete 360° scan of all the dihedral angles of the PEO using PM3.

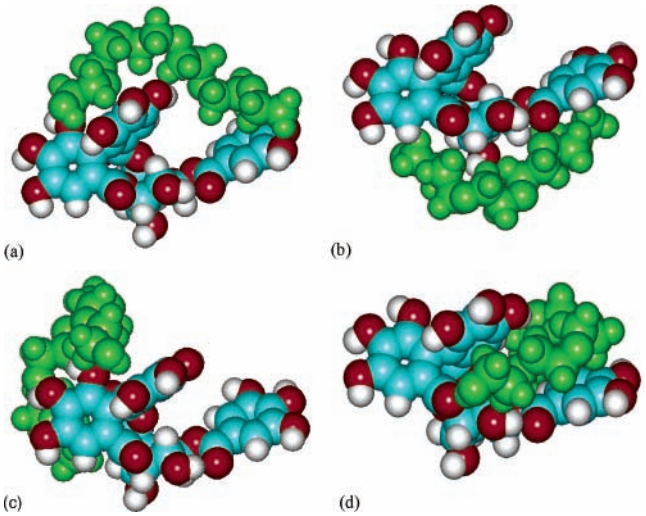

Figure 4. Complexes of $(PEO)_6$/corilagin-boat with different locations of the PEO hexamer: (a) top, (b) bottom, (c) side, and (d) inside the cavity of the cofactor corilagin-boat are shown.

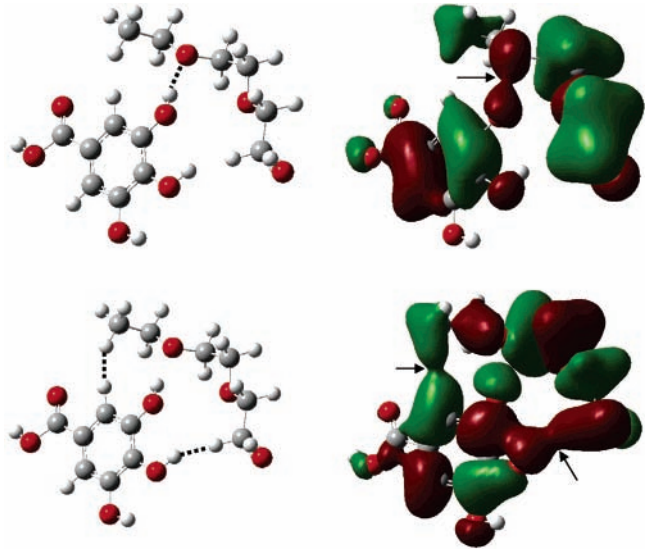

Figure 5. Molecular structure of $(PEO)_3$/gallic acid complex: the "H-bond" is dotted (top left). The molecular orbital, DLMO 13 (top right) with eigenvalue of −1.039 eV, shows a distinct "dumbbell" over the R−OH···O tri-atom region (arrow). The R−OH···H and R−CH···H interactions (bottom left), described by DLMO 18 (bottom right) with eigenvalue of −0.821 eV, also have the significant "dumbbell" appearance: all these interactions show a pinch in the MO and are weak regions.

PEO. The heat of formation of the hexamer of PEO at 0 K is $H_{f,0\,K} = -256.71$ kcal mol^{-1}. The hexamer ($(PEO)_6$) was used to ensure that the linear length is greater than the model cofactor size to minimize end-group effects (CH_3 and OH). However, in the case of the reference hydrogen-bonded complex, PEO/gallic acid, the ethylene oxide trimer ($(PEO)_3$) with $H_{f,0\,K} = -136.79$ kcal mol^{-1} was sufficient to avoid end effects.

$(PEO)_3$/Gallic Acid. Gallic acid, a subunit of the larger cofactors, which has hydrophilic OH's and a COOH group and a hydrophobic phenyl ring, was chosen as a model for studying the suggested hydrogen-bonding driving force. Gallic acid[18] (Figure 1b) has a global minimum with heat of formation $H_{f,0\,K} = -198.24$ kcal mol^{-1}. The $(PEO)_3$/gallic acid optimized from the PEO crystal structure, which has the oxygen inside, readily complexes at 0 K (Figure 5)

$$(PEO)_3 + \text{gallic acid} \rightleftharpoons (PEO)_3\text{/gallic acid} \qquad (3)$$

$$-136.79 + -198.24 \rightleftharpoons -341.41 \text{ kcal mol}^{-1}$$

since the complex ($H_{f,0\,K} = -341.41$ kcal mol^{-1}) is more stable than the sum of the reactants ($\sum(H_{f,0\,K}^{(PEO)_3} + H_{f,0\,K}^{gallic}) = -335.03$ kcal mol^{-1}). From eq 3, the enthalpies of association for the $(PEO)_3$/gallic acid complex at 0 and 298.15 K are −6.38 and −4.72 kcal mol^{-1}, respectively (Table 2), which is similar to a typical hydrogen-bond enthalpy[32] of about −5 kcal mol^{-1}. Steiner[33] refers to many different types of X−H···A hydrogen bonds which commonly occur in condensed phases and for which the dissociation energies span more than 2 orders of magnitude, from −0.2 to −40 kcal mol^{-1}. Any X−H···A interaction is called a hydrogen bond (a) if it constitutes a local bond and (b) if X−H acts as proton donor to A, and it is a directional molecular interaction.[33] $(PEO)_3$/gallic acid is assumed to have a hydrogen bond in the complex in Figure 5. The R−OH···O bond, with a bond length of 1.833 Å and an angle OH···O of 165.38° between a phenolic hydroxyl and an ether oxygen of PEO, is shown in the DLMO 13 as a pinched region of the wave function. Similar R−OH···O bond lengths and angles are found using density functional theory (DFT) and MP2 levels of theory.[34]

The PEO structure in aqueous solution would most likely have the ether oxygen outside to interact with the solvent. Therefore, it was decided to reoptimize the PEO structure. A more stable PEO conformer called $(PEO)_3^{scan}$ was obtained by performing a complete 360° scan of all the dihedral angles of the PEO trimer. This $(PEO)_3^{scan}$ does have the oxygen on the outside of the polymer (Figure 3, right). It readily complexes with the gallic acid at 0 K to give a more stable complex than the crystalline PEO structure with oxygen inside.

$$(PEO)_3^{scan} + \text{gallic acid} \rightleftharpoons (PEO)_3\text{/gallic acid} \qquad (4)$$

$$-142.23 + -198.24 \rightleftharpoons -347.19 \text{ kcal mol}^{-1}$$

since the complex ($H_{f,0\,K}^{complex} = -347.19$ kcal mol^{-1}) is more stable than the sum of the reactants ($\sum(H_{f,0\,K}^{(PEO)_3^{scan}} + H_{f,0\,K}^{gallic}) = -340.47$ kcal mol^{-1}). Equation 4 and thermochemical analysis show the enthalpy of association to be −6.72 and −5.42 kcal mol^{-1} at 0 and 298.15 K, respectively (Table 2). The enthalpies of association are interestingly quite similar, except that the $(PEO)_3^{scan}$/gallic acid complex is marginally (1.7%) more stable than the $(PEO)_3$/gallic acid complex.

TABLE 2: Thermochemistry[a] of the $(PEO)_3$/Gallic Acid Complexes at 0 and 298.15 K

PEO conformer[b]	$\Delta H_{0\,K}$ (kcal mol^{-1})	$\Delta G_{298\,K}$ (kcal mol^{-1})	$\Delta H_{298\,K}$ (kcal mol^{-1})	$T\Delta S_{298\,K}$ (kcal mol^{-1})	intermolecular R−OH···O[c]
$(PEO)_3$	−6.38	8.43	−4.72	−13.14	1
$(PEO)_3^{scan}$	−6.72	6.90	−5.42	−12.33	1
$(PEO)_3'$	−7.92		−6.03		1

[a] Scaling factor of 0.9761.[22] [b] $(PEO)_3'$ is very similar to $(PEO)_3$ and not $(PEO)_3^{scan}$. It is found by rotating PEO to remove all destabilizing H···H interactions, R−OH···H and R−CH···H (see text). [c] Judged by distance only.

The optimum PEO structure association lies between the $(PEO)_3$ crystalline structure and $(PEO)_3^{scan}$. It is important to use chemical understanding of the molecules when performing calculations: all possible complexes which are within 3 kcal mol^{-1} must be studied. The validity of this approach is shown by the fact that, starting with two very dissimilar PEO structures, $(PEO)_3$ and $(PEO)_3^{scan}$, very similar enthalpies of association of the minimized complexes are obtained.

The enthalpy of association of $(PEO)_3^{scan}$ /gallic acid at 298 K is identical to the experimental enthalpy of the hydrogen bond in the water dimer,[34] -5.4 ± 0.7 kcal mol^{-1}. With this enthalpy change, Hibbert and Emsley[35] would classify the $(PEO)_3$/gallic acid complexes as having a weak hydrogen bond. The calculated bond length, bond angle, and enthalpy change would lead Jeffry[30] to classify it as a "moderate hydrogen bond".

Although the enthalpy of association is negative and therefore promotes bonding, when two molecules associate there will also be an entropy change. From a frequency analysis of the calculations, the thermochemical analysis (Table 2) of $(PEO)_3$/gallic acid complexes shows that they will not form at room temperature (298.15 K) because of the entropy loss. It would be interesting to see whether the entropic effect can be lowered by taking the effect of the solvent into account, thus favoring a stable complex.

The wave functions and eigenvalues of the DLMOs describe the bonding between $(PEO)_3$ and gallic acid in the complex. Brion et al.[36] showed that molecular orbital theory is an accurate method to assess chemical bonding. Electron momentum spectroscopy (EMS) measurements and associated theoretical calculations, with evidence from frontier orbital theory and scanning tunneling microscopy (STM) experiments, show that delocalized canonical molecular orbitals (CMO) or Kohn−Sham orbital (KSO) densities provide a theoretically valid operational definition of orbitals and orbital electron densities.

Figure 5 shows DLMO 13 (top right), one of the 60 occupied DLMOs, as the only molecular orbital, which totally covers one phenolic hydroxyl and one ether oxygen of the PEO. The important aspect of this DLMO is that it covers the postulated hydrogen bond. There is a pinch in the DLMO at the postulated hydrogen bond which shows this to be the weakest region of electron density in the DLMO. Moreover, DLMO 18 (bottom right) shows two unusual interactions: R−OH···H and R−CH···H. The existence of such interactions has been reported in the literature.[37,38] However, these will be shown to be destabilizing interactions (see below).

The dumbbell section of the orbital is part of DLMO 13, and therefore, it is useful to determine the electron density (ρ) between the two specific atoms, using the density matrix. For a closed-shell system, the density matrix **P**, with elements $P_{\mu\nu}$,[39] described by eq 5, gives the contribution of the atomic orbitals (AO) in the occupied DLMO

$$P_{\mu\nu} = 2\sum_{i}^{occ} c_{\mu_i}^{*} c_{\nu_i} \qquad (5)$$

where c_{μ_i} and c_{ν_i} are the linear coefficients for the AOs μ and ν in the ith occupied DLMO.

The diagonal elements of the matrix give the electron density on a particular atom in the DLMO; the off-diagonal terms give the electron density shared by two atoms, reflecting their electronic interactions. Moreover, an electron density of 1 corresponds to a single covalent bond, and a weaker bond is indicated if ρ is lower than 1, such as in hydrogen bonds.

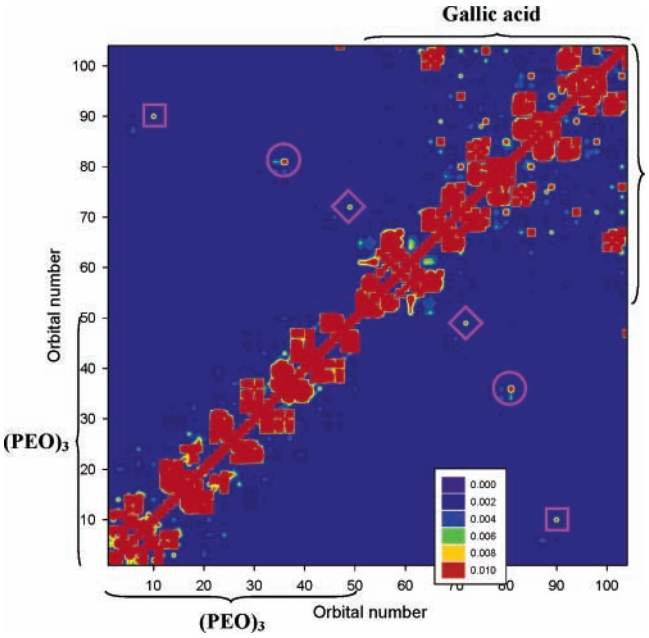

Figure 6. Electron density map of $(PEO)_3$/gallic acid complex. The R−OH···O interaction (○), shown in Figure 5, has a total electron density (ρ) of 0.0323 between the hydrogen proton of the phenolic group and the ether oxygen atom. The electron density of R−OH···H (□) and R−CH···H (◇) interactions are 0.0125 and 0.0121, respectively. The orange color represents the areas where the electron density is ≥0.01.

TABLE 3: Characterization of Intermolecular Bonds in $(PEO)_3$/Gallic Acid Complex

interatomic interactions	bond length (Å)	bond angle (°)	atomic orbitals in the MO	$\rho_{electron-density}$ (e/au^3)
$R_{phenol}-OH\cdots O_{ether}$	1.833	165.38	$1s^H-1s^O$	0.0056
			$1s^H-2p_x^O$	0.0045
			$1s^H-2p_y^O$	0.0210
			$1s^H-2p_z^O$	0.0012
			$\sum_\rho =$	0.0323
$R_{phenol}-OH\cdots H_{PEO}$	1.728	155.02	$1s^H-1s^H$	0.0125
$R_{phenol}-CH\cdots H_{PEO}$	1.720	148.67	$1s^H-1s^H$	0.0121

The x and y axes in Figure 6 represent the orbital number on each atom. The z axis perpendicular to the plane of the figure, represented here by the different colors, gives the electron density. The lower left segment of the electron density map from atomic orbital 49 down to 1 corresponds to the $(PEO)_3$ and the upper right to gallic acid from atomic orbital 50 up. The covalent bonds are located on the diagonal and in the two segments. The intramolecular bonds within these segments of the individual components, $(PEO)_3$ or gallic acid, describe intramolecular H-bonds or other similar interactions. The off-diagonal electron densities located in the upper left and lower segments describe the intermolecular interactions, hydrogen bonding, and similar interactions.

Considering the DLMO shown in Figure 5 (top), the electron density map in Figure 6, and the results of this figure tabulated in Table 3, the $R_{phenol}-OH\cdots O_{ether}$ interaction has a total electron density of 0.0323 e/au^3, of which 0.0210 is found between the 1s atomic orbital of the hydrogen proton of the phenolic group and the Py atomic orbital of the ether oxygen atom. The complex, $(PEO)_3$/gallic acid, therefore has an electron density which is larger than the electron density at the hydrogen bond critical point (ρ_{bcp}) as defined in an atom in a molecule program by Alkorta and Elguero[34] for the water dimer, 0.0231 e/au^3, calculated at the MP2/6-311++G** level.

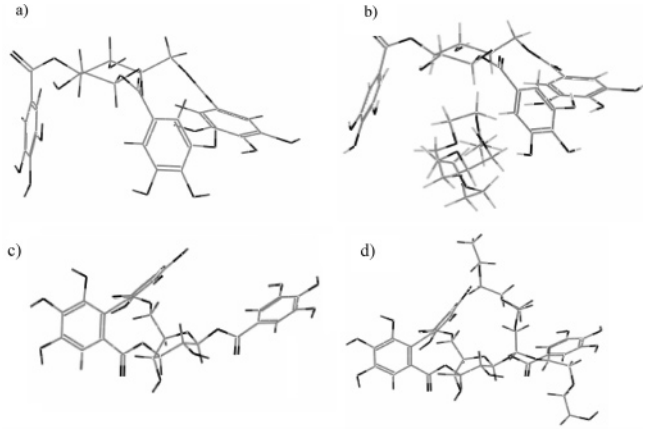

Figure 7. PM3 stick conformations (side view) of (a) TGG, (b) $(PEO)_6$/TGG, (c) corilagin-boat, and (d) $(PEO)_6$/corilagin-boat.

In the PEO/gallic acid complex, the $R_{phenol}-OH\cdots O_{ether}$ bond has a H···O bond length, *d*, of 1.833 Å and ln ρ of the total electron density, 0.0323 e/au^3, is −3.43. These results fit perfectly well with the linear 1n ρ_{bcp} versus *d* relationship, given by Steiner[33] as well as Alkorta and Elguero.[34] The density matrix has been used by Tretiak et al.[40] to study conjugated and aggregated molecules and was used to describe various bond types.

The electron density map shows two additional interactions in the $(PEO)_3$/gallic acid complex, Figure 5 (bottom) and Figure 6 (indicated by □ and ◇).

The interactions R−OH···H (□) and R−CH···H (◇) have been suggested as possible hydrogen bonds, because the two hydrogen atoms share the same electron density. Table 3 shows that these H···H bonds in R−OH···H and R−CH···H have smaller electron densities (0.0125 and 0.0121) than the R−OH···H (0.0323) interaction, even though the bond lengths are shorter. Klooster et al.[38] reported that H···H distances are typically 1.7−2.2 Å for M−H···H−N bonds, where M stands for metal, compared with the present results 1.728 and 1.720. Because the R−OH···O interaction has a larger electron density than either R−OH···H or R−CH···H, the R−OH···O interaction is about three times stronger. Consequently, additional calculations were performed to study these interactions energetically, because they occur in many of the complexes. The R−OH···H and R−CH···H interactions were removed from $(PEO)_3$/gallic acid, and the enthalpy of formation was calculated to be 0.45%, or −1.54 kcal mol^{-1} more stable than the complex containing the R−OH···H and R−CH···H. The enthalpies of association were −7.92 and −6.03 kcal mol^{-1} at 0 and 298.15 K, respectively (Table 2). The electron density (ρ) for the R−OH···O interaction, when the R−OH···H and R−CH···H were removed, increased to 0.0337 from 0.0323. This proves that these R−OH···H (□) and R−CH···H (◇) interactions are destabilizing. It is necessary to carefully search the potential energy surface of the complexes to avoid such destabilizations.

$(PEO)_6$/TGG. To consider the complexing of large cofactors which contain several gallic acid subgroups, it becomes necessary to use $(PEO)_6$ to avoid effects from CH_3 and OH end groups. At 0 K, TGG has three conformers,[18] chair, semi-tripod, and tripod, with heats of formation ($H_{f,0\,K}$) of −666.66, −668.48, and −670.42 kcal mol^{-1}, respectively (Table 1). The chair, semi-tripod, and tripod conformers are used to study the interactions between TGG and PEO (Figure 7a,b). Table 4 shows that the enthalpy of association ($\Delta H_{0\,K}$) for these conformers varies from −12.50 to −17.36 kcal mol^{-1}, and thus, these complexes form at 0 K. The $(PEO)_6$/TGG-tripod has the most stable conformation, $H_{f,0\,K} = -944.49$ kcal mol^{-1}, and the lowest enthalpy of association, $\Delta H_{0\,K} = -17.36$ kcal mol^{-1}. The complexes were recalculated at 298.15 K, (cf. Table 5). Included in the calculations were vibrational, rotational, translational, and electronic entropies and energies. The results show that the $(PEO)_6$/TGG complexes will not form at room temperature, because high entropy prevents complexation. The TGG-tripod conformer still has the most stable enthalpy of association, $\Delta H_{298\,K} = -13.82$ kcal mol^{-1}.

TABLE 4: Heats of Formation and the Enthalpy of Association for the $(PEO)_6$/Cofactor Complexes at 0 K

complexes PEO/cofactor	conformer	$H_{f,0\,K}$ (kcal/mol)	$\Delta H_{f,0\,K}$ (kcal/mol)	intra-R−OH···O[a]	inter-R−OH···O[a]
$(PEO)_6$/TGG	chair	−938.29	−14.92	0	1
$(PEO)_6$/TGG	semi-tripod	−937.69	−12.50	0	1
$(PEO)_6$/TGG	tripod	−944.49	−17.36	1	1
$(PEO)_6$/corilagin	boat	−922.18	−15.23	1	4[b]
$(PEO)_6$/corilagin	boat	−921.85	−14.90	1	1
$(PEO)_6$/corilagin	skew-boat	−928.94	−20.00	1	1
$(PEO)_6$/corilagin	chair	−912.79	−18.51	0	3
$(PEO)_6$/R1R3	skew-boat	−913.48	−12.64	1	1
$(PEO)_6$/R1R6	skew-boat	−932.19	−17.96	2	1

[a] Judged by distance only. [b] One bond is of the R−CH···O type.

TABLE 5: Thermochemistry for the Association of PEO Hexamer and Cofactors at 298.15 K

complexes cofactor/PEO[a]	conformer	$\Delta G_{298\,K}$ (kcal mol^{-1})	$\Delta H_{298\,K}$ (kcal mol^{-1})	$T\Delta S_{298\,K}$ (kcal mol^{-1})	inter-R−OH···O[b]
[1] $(PEO)_6$/TGG	chair	10.05	−12.83	−22.88	1
[2] $(PEO)_6$/TGG	semi-tripod	17.66	−9.98	−27.64	1
[3] $(PEO)_6$/TGG	tripod	9.24	−13.82	−23.06	1
[4] $(PEO)_6$/corilagin	boat	14.13	−12.45	−26.58	4[c]
[5] $(PEO)_6$/corilagin	boat	10.62	−12.25	−22.87	1
[6] $(PEO)_6$/corilagin	skew-boat	7.73	−16.78	−24.50	1
[7] $(PEO)_6$/corilagin	chair	11.46	−16.05	−27.51	3
[8] $(PEO)_6$/R1R3	skew-boat	11.49	−10.03	−21.52	1
[9] $(PEO)_6$/R1R6	skew-boat	11.66	−14.92	−26.58	1

[a] The numbering of complexes is used in Table 9 and Figure 10. [b] Judged by distance only. [c] One bond is of the R−CH···O type.

$(PEO)_6$/Corilagin. Corilagin, which has two phenolic rings (R3R6) joined, has two boat conformers,[18] boat and skew-boat, with heats of formation of −650.24 and −652.23 kcal mol^{-1}, respectively, and a much less stable chair conformer[18] with heat of formation of −637.57 kcal mol^{-1} (Table 1). All three conformers were used to study the interactions with PEO (Figure 7c,d). Tables 4 and 5 show that the $(PEO)_6$/corilagin skew-boat complex is the most stable with enthalpies of association: at 0 K, $\Delta H_{0\,K} = -20.00$, and at 298.15 K, $\Delta H_{298\,K} = -16.78$ kcal mol^{-1}. The $(PEO)_6$/corilagin-boat complex shows no dependence of the heat of formation ($\Delta H_{0\,K}$) on the number of intermolecular H-bonds. For example, for a decrease from 4 to 1 hydrogen bonds, the enthalpy of association $\Delta H_{0\,K}$ changes from −15.23 to −14.90 kcal mol^{-1} (Table 4). At 298.15 K, $\Delta H_{298\,K}$ values are even closer: −12.45 and −12.25 kcal mol^{-1}, respectively. Three of these bonds are of the R−OH···O type (Figure 8), while one bond is of the R−CH···O type (Table 6). It is even possible to form $(PEO)_6$/corilagin complexes with a somewhat smaller enthalpy of association, which contains no H-bonds.

The results for the $(PEO)_6$/corilagin are the same as for the $(PEO)_6$/TGG complexes. The complexes do not form at room temperature, because $T\Delta S$ is too large, making $\Delta G > 0$ ($\Delta G = \Delta H - T\Delta S$). The PM3 stick conformation of TGG, corilagin, and their complexes with $(PEO)_6$ are shown in Figure 7.

The behavior of PEO/cofactor complexes is different from stable systems studied by Alkorta and Elguero,[34] who found

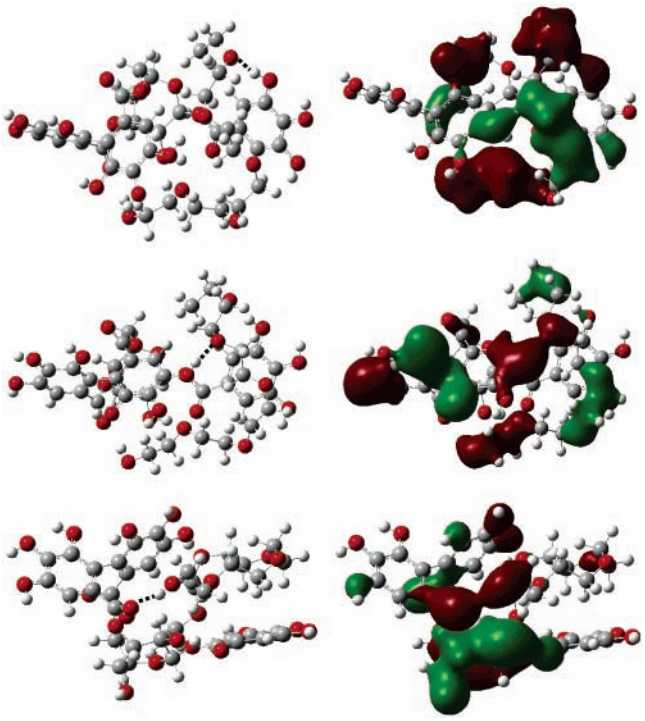

Figure 8. Molecular structure of $(PEO)_6$/corilagin-boat complex showing three R−OH···O bonds (dotted lines), and the corresponding DLMOs: 9 (top right), 11 (center right), and 17 (bottom right), with eigenvalues of −1.453, −1.427, and −1.351 eV, respectively.

that the interaction energy follows an exponential relationship with respect to the number of R−OH···O bonds.

TABLE 6: Bond Characterization in $(PEO)_6$/Corilagin-Boat Complex

interatomic interactions	inter or intra H-bond	bond length (Å)	bond angle (°)	ρ^a (e/au^3)
$R_{phenol}-OH\cdots O_{ether}$	inter	1.818	163.84	0.0310
$R_{phenol}-OH\cdots O_{ether}$	inter	1.820	165.76	0.0311
$R_{PEO}-OH\cdots O_{carbonyl}$	inter	1.846	168.74	0.0215
$R_{sugar}-OH\cdots O_{carbonyl}$	intra	1.812	154.66	0.0341
$R_{PEO}-CH\cdots O_{sugar}$	inter	1.872	175.44	0.0205
$R_{PEO}-CH\cdots H_{phenol}$	inter	1.714	150.67	0.0130
$R_{PEO}-CH\cdots H_{phenol}$	inter	1.755	138.41	0.0114

$^a\ \rho = \sum[\rho(1s^H-1s^O) + \rho(1s^H-2p_x^O) + \rho(1s^H-2p_y^O) + \rho(1s^H-2p_z^O)$.

Figure 8 shows DLMOs 9, 11, and 17, out of 174 occupied DLMOs, which totally cover one hydroxyl and an ether oxygen of the PEO, R−OH···O, traditionally described as a hydrogen bond. Considering DLMO 11 (center right), only a part of the orbital is found to cover the H···O atoms. The electron density on the two atoms H···O in the R−OH···O part of the molecular complex occurs in many DLMOs: 3, 4, 6, 9, 11, 12, 17, and 21, with eigenvalues of −1.562, −1.527, −1.505, −1.453, −1.427, −1.417, −1.351, and −1.329 eV, respectively. Notice again the characteristic "pinch" of the orbitals in the R−OH···O regions.

Figure 9 and Table 6 show three types of interaction: (i) R−OH···O, (ii) R−CH···O, and (iii) R−CH···H. R−OH···O is the traditional hydrogen bond. It has been suggested that the R−CH···O has similar characteristics to R−OH···O and can be treated as a true hydrogen bond.[41,42] Table 6 shows that the R−CH···O has a similar electron density, $\rho = 0.0215$, to the $R_{PEO}-OH\cdots O_{carbonyl}$ $\rho = 0.0215$ interaction, but with a larger

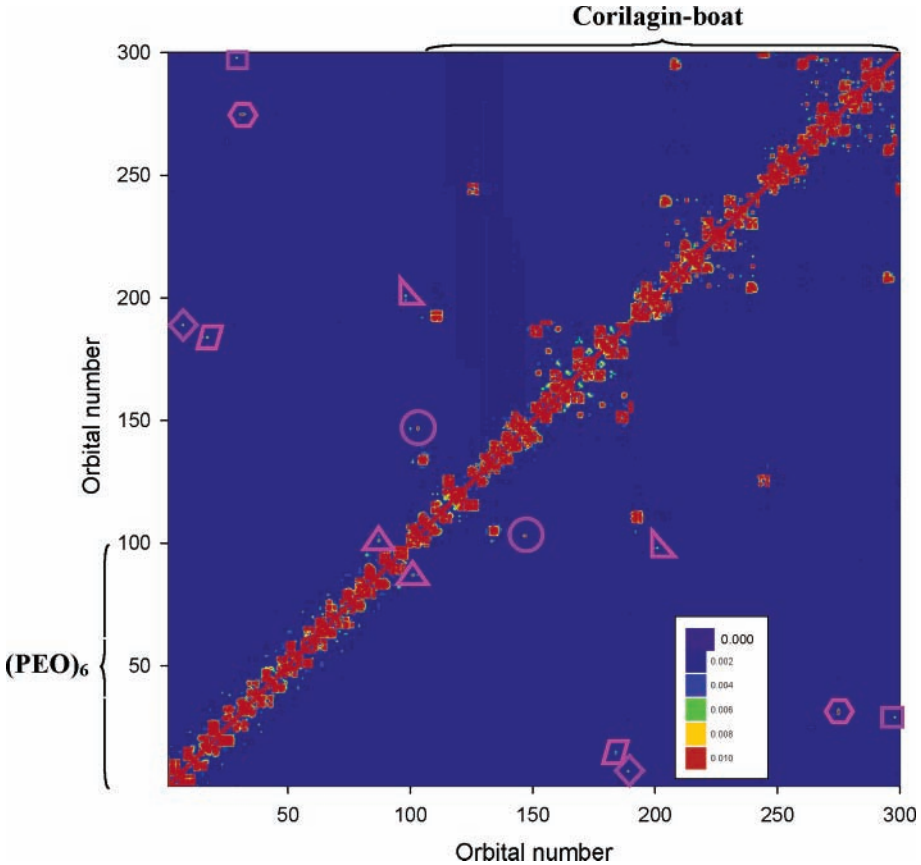

Figure 9. Electron density map of $(PEO)_6$/corilagin-boat complex. The molecular interaction electron densities are as follows: 0.0310 ($R_{phenol}-OH\cdots O_{ether}$, □), 0.0311 ($R_{phenol}-OH\cdots O_{ether}$, ⬡), 0.0215 ($R_{PEO}-OH\cdots O_{carbonyl}$, right triangle), 0.0341 ($R_{sugar}-OH\cdots O_{carbonyl}$, ○), 0.0205 ($R_{PEO}-CH\cdots O_{sugar}$, △), 0.0130 ($R_{PEO}-CH\cdots H_{phenol}$, ◇), and 0.0114 ($R_{PEO}-CH\cdots H_{phenol}$, □) (Table 6). The orange color represents the areas where the electron density is ≥0.01. $(PEO)_6$ is described by orbitals numbered 1 to 98, and corilagin-boat is described by orbitals 99 to 300.

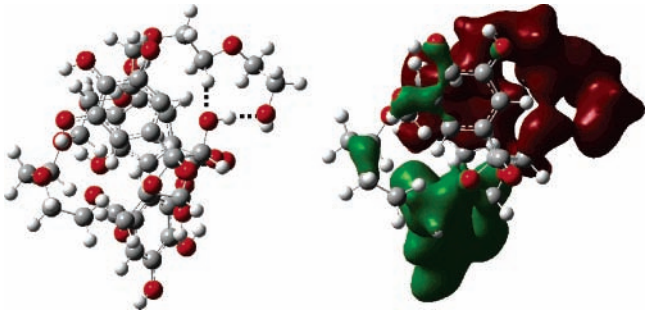

Figure 10. PM3 optimized molecular structure of $(PEO)_6$/corilagin-chair complex shows R−OH···O and R−CH···O bonds (dotted lines, left) and DLMO 6 (right), covering both R−OH···O and R−CH···O, with eigenvalue −1.505 eV. Notice that the two hydrogen bonds, R−OH···O and R−CH···O, are shown by significant "pinches" in the DLMO, showing a very weak density between the H···O atoms.

bond length, 1.872 Å compared to 1.846 Å. These results are similar to the ideas of Gu et al.,[42] who suggested that R−CH···O bonds are usually weaker than conventional hydrogen bonds but their binding energy would die off more gradually as the hydrogen bond distance is stretched. Consequently, an R−CH···O bond may even be stronger than the R−OH···O interaction in particular intermolecular systems.

In the present $(PEO)_6$/corilagin-boat complex, an interesting and unsual H···H type of interaction has been found. These two R−CH···H interactions have a lower electron density than R−OH···O, even though the bond lengths are shorter (Table 6). Traditionally, shorter hydrogen bond lengths give a more stable hydrogen bond.[33] Consequently, bond length can be correlated with electron density only when comparing identical types of hydrogen bonds.[33,34] These R−CH···H interactions have been shown to destabilize the PEO/gallic acid complex, which becomes more stable when the R−CH···H are eliminated by rotating the gallic acid relative to PEO around the true R−OH···O hydrogen bond. However, these very large PEO/cofactor complexes are in their global minima, and the destabilizing effect of R−CH···H is energetically smaller.

In a chain with two adjacent R−OH···O and R−CH···O bonds in the $(PEO)_6$/corilagin-chair complex shown in Figure 10, the H···O atoms are covered by two DLMOs, 4 and 6, one of which is shown in Figure 10 (right). It has been suggested that both bonds in Y−H···X−H···A become stronger.[33,43] The so-called polarization-enhanced hydrogen bonding[33] occurs in the $(PEO)_6$/corilagin-chair complex, as shown by the DLMOs.

$(PEO)_6$/(R1R3) and $(PEO)_6$/R1R6. Table 4 shows $(PEO)_3$/(R1R3) has a higher enthalpy of formation ($H_{f,0\,K} = -913.48$ kcal mol^{-1}) than $(PEO)_3$/R1R6 ($H_{f,0\,K} = -932.19$ kcal mol^{-1}). $(PEO)_3$/R1R6 can form a more stable complex than any of the corilagin conformers complexes at 0 K, between $H_{f,0\,K} = -912.79$ and -928.94 kcal mol^{-1}. Interestingly, $(PEO)_3$/R1R6 does not have a lower enthalpy of association. It would be interesting to see whether R1R6 could be used as a cofactor, because of the large enthalpy of formation of the $(PEO)_3$/R1R6 complex. However, the entropic effect is still predominant (Table 5).

Since all PEO/cofactor complexes studied so far do not form at room temperature, one interesting question is, would there be any possibility that the entropic effect could be overcome by having more PEOs complexing with a single cofactor? In industrial applications, PEO has a much higher molecular weight than the one used in the modeling, and consequently, the possibility of one part of the PEO being complexed with the cofactor from above and another part from below, to give a sandwich-type complex, was studied.

$(PEO)_6$/TGG/$(PEO)_6$. The thermochemistry of the complexes when a cofactor is sandwiched between two PEO hexamers was calculated to investigate the possibility that a cofactor could induce PEO aggregation and overcome the entropic effect. The association between a $(PEO)_6$/cofactor complex (Table 4) and another PEO hexamer to generate a larger complex, with more possibilities for bonding, is

$$(PEO)_6/TGG + (PEO)_6 \rightleftharpoons (PEO)_6/TGG/(PEO)_6 \quad (6)$$

The conformation of the additional PEO hexamer was varied to increase the number of bonds, to maximize the stability of the assembly, to give the energetically ($H_{f,0\,K}$) most stable complex. It was expected that the enthalpy of association would be about twice that reported in Tables 4 and 5. Table 7 shows that, when cofactor associates with two PEO hexamers at 0 K, the enthalpy of association increases by factors of 1.81 for the chair, 2.00 for the semi-tripod, and 1.81 for the tripod conformers relative to the values in Table 4. However, it is important to note that this increase in the enthalpy of association occurs even though the number of intermolecular R−OH···O and R−CH···O bonds (a) stayed constant for chair and semi-tripod, but (b) increased from 1 to 2 for the tripod conformer.

The enthalpy of association almost doubled at 0 K for the same number of intermolecular R−OH···O and R−CH···O bonds, indicating that there is no correlation between the enthalpy of association and the number of H-bonds. Similar trends are observed at 298.15 K (Table 8): The enthalpy of association increases by factors of 1.77 for the chair, 1.97 for the semi-tripod, and 1.85 for the tripod conformers relative to the values in Table 5. The $(PEO)_6$/TGG-tripod/$(PEO)_6$ is the most stable complex and has the lowest enthalpy of association at both 0 and 298.15 K. The larger complexes (Table 8) behave similarly to the smaller complexes (Table 5). These complexes all have large $T\Delta S$ values, which prevent association. Interestingly, the $(PEO)_6$/TGG semi-tripod/$(PEO)_6$ complex has a particularly high $T\Delta S$, which reflects the very tight packing of the complex.

$(PEO)_6$/corilagin/$(PEO)_6$. When corilagin conformers associate with one and two PEO hexamers, Tables 4 and 7, the

TABLE 7: Heats of Formation and Association Enthalpies for the $(PEO)_6$/Cofactor/$(PEO)_6$ Complexes at 0 K

complexes cofactor/PEO	conformers	$H_{f,0\,K}$ (kcal mol^{-1})	$\Delta H_{0\,K}$ (kcal mol^{-1})	intramolecular R−OH···O[a]	intermolecular R−OH···O[a]
$(PEO)_6$/TGG/$(PEO)_6$	chair	−1207.08	−27.00	0	1
$(PEO)_6$/TGG/$(PEO)_6$	semi-tripod	−1206.85	−24.95	0	1
$(PEO)_6$/TGG/$(PEO)_6$	tripod	−1215.26	−31.42	1	2
$(PEO)_6$/corilagin/$(PEO)_6$	boat	−1188.72	−25.06	1	4[b]
$(PEO)_6$/corilagin/$(PEO)_6$	skew-boat	−1193.84	−28.19	1	1
$(PEO)_6$/corilagin/$(PEO)_6$	chair	−1177.24	−26.25	0	3
$(PEO)_6$/R1R3/$(PEO)_6$	skew-boat	−1182.03	−24.48	1	2
$(PEO)_6$/R1R6/$(PEO)_6$	skew-boat	−1197.10	−26.16	2	1

[a] Judged by distance only. [b] One bond is of the R−CH···O type.

TABLE 8: Thermochemistry for the Association of (PEO)$_6$/Cofactor/(PEO)$_6$ Complexes at 298.15 K

complexes	conformers	$\Delta G_{298\,K}$ (kcal/mol)	$\Delta H_{298\,K}$ (kcal/mol)	$T\Delta S_{298\,K}$ (kcal/mol)	intermolecular R−OH···O[a]
(PEO)$_6$/TGG/(PEO)$_6$	chair	18.66	−22.75	−41.41	1
(PEO)$_6$/TGG/(PEO)$_6$	semi-tripod	32.92	−19.65	−52.57	1
(PEO)$_6$/TGG/(PEO)$_6$	tripod	22.08	−25.57	−47.65	2
(PEO)$_6$/corilagin/(PEO)$_6$	boat	23.30	−20.44	−43.74	4[b]
(PEO)$_6$/corilagin/(PEO)$_6$	skew-boat	18.14	−23.32	−41.46	1
(PEO)$_6$/corilagin/(PEO)$_6$	chair	23.22	−21.62	−44.84	3
(PEO)$_6$/R1R3/(PEO)$_6$	skew-boat	21.18	−20.72	−41.90	2
(PEO)$_6$/R1R6/(PEO)$_6$	skew-boat	21.29	−21.31	−42.60	1

[a] Judged by distance only. [b] One bond is of the R−CH···O type.

enthalpy of association at 0 K increases by factors of 1.65 for the boat, 1.41 for the skew-boat, and 1.42 for the chair conformers. Similar trends are observed at 298.15 K: The enthalpy of association increases by factors of 1.64 for the boat, 1.39 for the skew-boat, and 1.35 for the chair conformers. Again, no association occurs at room temperature because of high entropy (Tables 5 and 8). Again, there is no correlation between the number of intermolecular H− bonds and the enthalpy of association for the corilagin conformers.

(PEO)$_6$/R1R3/(PEO)$_6$ and (PEO)$_6$/R1R6/(PEO)$_6$. These two model corilagin-type cofactors give a (PEO)$_6$/R1R6/(PEO)$_6$ complex more stable than the (PEO)6/R1R3/(PEO)6 complex, having $H_{f,0\,K}$ of −1197.10 compared to −1182.03 kcal mol^{-1} (Table 7).

Similarly to the corilagin complexes, there is no association at room temperature because of high entropy (Table 8). Again, there is no correlation between the number of intermolecular H− bonds and the enthalpy of association for the conformers.

Change in Enthalpy (ΔH_f) And Change in Entropy (ΔS). The relationship between the change in enthalpy (ΔH_f) and the change in entropy (ΔS) is discussed extensively in the literature. Williams et al.[44,45] showed that for the gas phase the change in enthalpy of association increases approximately linearly with the change in entropy, with $\Delta H = 0$ at $T\Delta S = 0$.[44] In the present work, the theoretical change in enthalpy of association plotted against the theoretical change in entropy between PEO and its cofactors (Tables 2, 5, and 8) is also assumed to pass through the origin. The (PEO)$_6$/cofactor/(PEO)$_6$ complexes have larger theoretical enthalpies of association than the (PEO)$_6$/cofactor complexes because of additional intermolecular interactions from the second PEO (Figure 11).

These results show a relatively good correlation, $R^2 = 0.841$, between calculated enthalpy and calculated entropy change. However, a detailed analysis for the larger PEO/cofactor complexes gives more insight, showing that the cofactor conformation plays a significant role in the interaction with the very flexible PEO molecule. The cofactor affects the PEO conformation, and vice versa (Figure 12).

Such an analysis gives additional information about the interactions between molecules forming complexes. While this idea has been developed for complexes which only form at 0 K, nevertheless it would be useful to show the specificity of the cofactors in the plots of Williams et al.[44−45] Corilagin skew-boat gives the largest change in enthalpy of association for a given entropy change, with the highest slope of 0.59 (Figure 12). The TGG semi-tripod conformer complex has the smallest enthalpy change for a given entropy change, with a slope of 0.37. The corilagin boat shows a perfectly linear behavior with a slope of 0.47. R1R3 and R1R6 show similar behavior and were combined in a single line. The idea that the complexes do not form at room temperature, because the loss of entropy exceeds the enthalpy increase, is clearly shown in Figures 11 and 12.

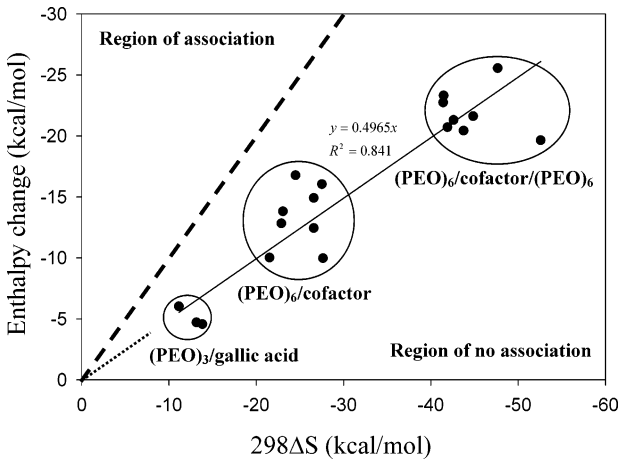

Figure 11. Change in calculated enthalpy as a function of the change in calculated entropy at 298.15 K, for gas-phase interactions of PEO/cofactor complexes. The correlation factor R^2 was calculated on the assumption that the line goes through the origin.[44] The dotted line is the boundary between regions in which association occurs or is absent.

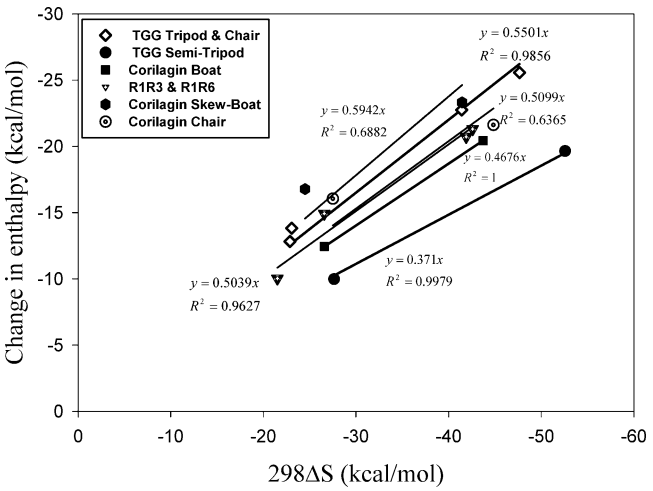

Figure 12. Change in calculated enthalpy as a function of the change of calculated entropy at 298.15 K, for gas-phase interactions of PEO/cofactor complexes. The correlation factors R^2 were calculated on the assumption that all the lines go through the origin.[44]

The relative contributions of PEO and the cofactor to the enthalpy and entropy changes are analyzed for the (PEO)$_6$/cofactor complexes (Table 9). The enthalpy and entropy changes mainly arise from PEO (Table 9). The negative values in Table 9 signify that the reactant ($\Delta H_{cofactor}$ and/or ΔH_{PEO}) conformers are more stable after complexation than before, implying that the PEO and the cofactors were not in a global energy minimum before complexation. The change A → A′ is very important (Table 9). All the results are calculated from eq 1. It would be

TABLE 9: Changes in Enthalpy and Entropy (in kcal mol^{-1}) Arising from the Individual Components (Cofactor and PEO) of $(PEO)_6$/Cofactor Complexes at 298.15 K

complex[a]	$\Delta H_{cofactor}$	ΔH_{PEO}	$\Delta H_{association}$ [b]	$T\Delta S_{cofactor}$	$T\Delta S_{PEO}$	$T\Delta S_{association}$ [b]
1	−0.43	0.41	−12.83	−3.31	−2.44	−22.88
2	4.97	2.00	−9.98	1.14	−5.80	−27.64
3	1.74	−4.59	−13.82	0.95	−5.30	−23.06
4	1.81	−3.42	−12.45	−0.64	−5.50	−26.58
5	1.93	−3.69	−12.25	0.22	−4.36	−22.87
6	−0.96	−3.67	−16.78	−1.88	−4.60	−24.50
7	0.12	1.44	−16.05	−0.87	−1.91	−27.51
8	−0.56	−3.72	−10.03	−0.13	−3.22	−21.52
9	1.99	−4.61	−14.92	−1.86	−4.72	−26.58

[a] Complexes listed in Table 5. [b] Values extracted from Table 5.

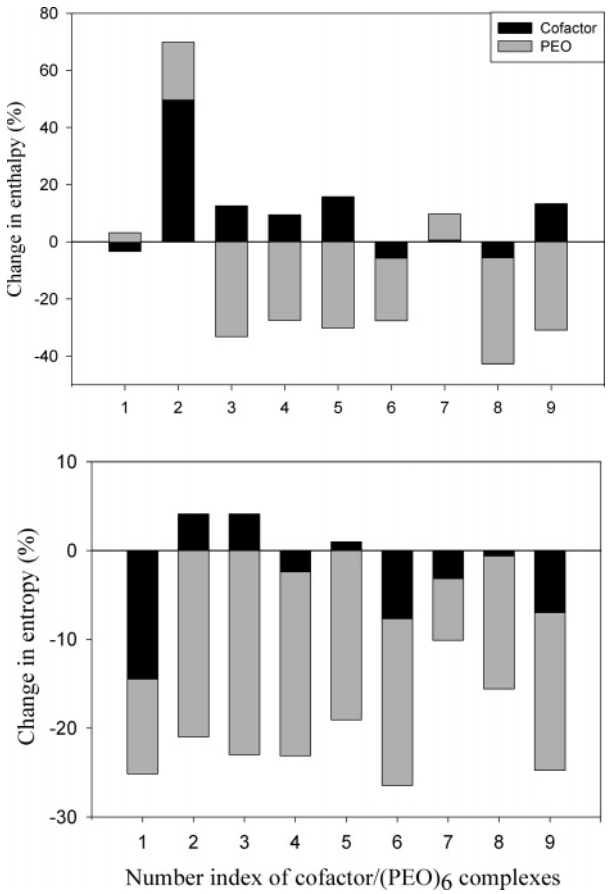

Figure 13. Change in enthalpy and entropy at 298.15 K arising from the individual components (cofactor and $(PEO)_6$) for gas-phase complexes. Number index refers to Table 5.

interesting to separate and analyze all the experimental results of Williams et al.[44] using this analytical technique.

Only for system 2 ($(PEO)_6$/TGG semi-tripod) does the change in enthalpy, caused by the cofactor and PEO combined, equal 70% of the total enthalpy change ($*\Delta H_{association}$) (Figure 13 top). Otherwise, the enthalpy change due to cofactor and PEO combined is lower than 45% of the total enthalpy change. The entropy change is mainly due to PEO, but the effect of cofactor and PEO combined is usually below 25% of the total entropy change ($*T\Delta S_{association}$) (Figure 13 bottom).

Conclusions

PEO/gallic acid, PEO/TGG, and PEO/corilagin complexes form at 0 K, while they do not associate at room temperature because the entropy loss is larger than the gain in enthalpy. When TGG conformers associate with one to two PEO hexamers at 0 K, the enthalpy of association increases by factors of 1.81 for the chair, 2.00 for the semi-tripod, and 1.81 for the tripod conformers, but the number of R−OH···O and R−CH···O bonds stayed constant for the chair and semi-tripod, respectively. Moreover, the $(PEO)_6$/corilagin-boat complex shows no significant difference in the enthalpy of association when the number of H-bonds decreased from 4 to 1. Consequently, there is no correlation between the number of intermolecular R−OH···O and R−CH···O bonds and the heat of formation or the enthalpy of association at 0 and 298.15 K.

Linear relationships between the change in enthalpy and the change in entropy show the specificity of the cofactors when interacting with the very flexible PEO. DLMOs were used to show the molecular bonding regions. The electron density map supports the R−OH···H and R−CH···H interactions for the $(PEO)_3$/gallic acid and larger PEO/cofactor complexes. The interactions R−OH···H and R−CH···H are found to be destabilizing with electron densities ranging from 0.0114 to 0.0130.

Even though bond lengths, bond angles, delocalized molecular orbitals, and electron densities for the PEO/cofactor complexes are consistent with the definition of hydrogen bonds, the number of R−OH···O and R−CH···O bonds does not correlate with the enthalpy of association, indicating that the bonding mechanism for these systems is the sum of many small contributions of many delocalized orbitals.

Since these complexes do not hold together at 298.15 K, the whole question of hydrogen bonding between phenolic cofactors and PEO becomes of academic interest and of no practical significance. It is interesting that insights into the complexes has been possible even though they do not form in the absence of salt. With salt, complexation is observed.[46] In subsequent paper, the hydrophobic and hydrophilic interactions will be reported, including the effects of the size of PEO, the possibility of end group effects, and whether phenolic hydroxyl groups in cofactors are necessary.[47]

Acknowledgment. The authors would like to acknowledge Cecile Malardier-Jugroot, Dr. Adam Dickie, and Dr. Felaniaina Rakotondradany for valuable assistance and discussions. We would also like to acknowledge Dr. Julie Giasson and Dr. Christian Lauzier for providing the crystal structure of PEO. Financial support from Paprican and NSERC for an Industrial Research Chair is also acknowledged.

References and Notes

(1) Lindström, T.; Glad-Normark, G. Flocculation of Latex and Cellulose Dispersions by Means of Transient Polymer Networks. *Colloids Surf.* **1984**, *8*, 337−351.

(2) Pelton, R.; Xiao, H.; Hamielec, A. Retention Mechanisms for Two-Component Systems Based on Phenolic Resins and PEO or New PEO−Copolymer Retention Aids. *J. Pulp Paper Sci.* **1996**, *22* (12), J475−J485.

(3) van de Ven, T. G. M.; Alince, B. Association-Induced Polymer Bridging: New Insights into the Retention of Fillers with PEO. *J. Pulp Paper Sci.* **1996**, *22* (7), J257−J263.

(4) Takase, H.; van de Ven, T. G. M. Effect of a cofactor on the polymer bridging of latex particles to glass by poly(ethylene oxide). *Colloid Surf., A* **1996**, *118*, 115−120.

(5) van de Ven, T. G. M. Mechanisms of Fines and Filler Retention with PEO/Cofactor Dual Retention Aid Systems. *J. Pulp Paper Sci.* **1997**, *23* (9), J447−J451.

(6) Carignan, A.; Garnier, G.; van de Ven, T. G. M. The Flocculation of Fines by PEO/Cofactor Retention Aid Systems. *J. Pulp Paper Sci.* **1998**, *24* (3), 94−99.

(7) van de Ven, T. G. M. Assciation-Induced Polymer Bridging by Poly(Ethylene Oxide)-Cofactor Flocculation Systems. *Adv. Colloid Interface Sci.* In press.

(8) Stack, K. R.; Dunn, L. A.; Roberts, N. K. Study of the Interaction Between Poly(Ethylene Oxide) and Phenol-Formaldehyde Resin. *Colloids Surf.* **1991**, *61*, 205−218.

(9) Pelton, R.; Xiao, H.; Brook, M. A.; Hamielec, A. Flocculation of Polystyrene Latex with Mixtures of Poly(*p*-vinylphenol) and Poly(ethylene oxide). *Langmuir* **1996**, *12*, 5756−5762.

(10) Zhang, X.; Takegoshi, K.; Hikichi, K. Composition Dependence of the Miscibility and Phase Structure of Amorphous/Crystalline Polymer Blends as Studied by High-Resolution Solid-State ^{13}C NMR Spectroscopy. *Macromolecules* **1992**, *25*, 2336−2340.

(11) Cong, R.; Bain, A. D.; Pelton, R. An NMR Investigation of the Interaction of Poly(ethylene oxide) with Water-Soluble Poly(vinyl phenol-*co*-potassium styrene sulfonate). *J. Polym. Sci., Part B: Polym. Phys.* **2000**, *38*, 1276−1284.

(12) Goto, S.; Miyanishi, T.; Pelton, R. Novel Cofactors/PEO Flocculation Systems for Colloidal Suspensions. *Nord. Pulp Pap. Res. J.* **2000**, *15* (5), 395−399.

(13) Lu, C.; Pelton, R.; Valliant, J.; Bothwell, S.; Stephenson, K. Colloidal Flocculation with Poly(ethylene oxide)/Polypeptide Complexes. *Langmuir* **2002**, *18*, 4536−4538.

(14) Malardier-Jugroot, C.; Spivey, A. C.; Whitehead, M. A. Study of the influence of the non-pyridyl nitrogen hybridisation on the stability of axially chiral analogues of 4-(dimethylamino)pyridine (DMAP). *THEOCHEM* **2003**, *623*, 263−276.

(15) Stewart, J. J. P. Optimization of Parameters for Semiempirical Methods I. Method. *J. Comput. Chem.* **1989**, *10* (2), 209−220.

(16) Stewart, J. J. P. Optimization of Parameters for Semiempirical Methods II. Applications. *J. Comput. Chem.* **1989**, *10* (2), 221−264.

(17) Rakotondradany, F.; Whitehead, M. A.; Lebuis, A. M.; Sleiman, H. F. Photoresponsive Supramolecular Systems: Self-Assembly of Azodibenzoic Acid Linear Tapes and Cyclic Tetramers. *Chem.−Eur. J.* **2003**, *9*, 4771−4780.

(18) Gaudreault, R.; Whitehead, M. A.; van de Ven. T. G. M. Molecular Modeling of Polye(ethylene oxide) Model Cofactors; 1,3,6-Tri-O-Galloyl-β-D-Glucose and Corilagin. *J. Mol. Model.* **2002**, *8*, 73−80.

(19) *The Merck Index*, 13th ed.; Merck & Co.: Rahway, NJ, 2001; pp 1615−1616.

(20) Frisch, M. J.; Trucks, G. W.; Schlegel, H. B.; Scuseria, G. E.; Robb, M. A.; Cheeseman, J. R.; Zakrzewski, V. G.; Montgomery, J. A., Jr.; Stratmann, R. E.; Burant, J. C.; Dapprich, S.; Millam, J. M.; Daniels, A. D.; Kudin, K. N.; Strain, M. C.; Farkas, O.; Tomasi, J.; Barone, V.; Cossi, M.; Cammi, R.; Mennucci, B.; Pomelli, C.; Adamo, C.; Clifford, S.; Ochterski, J.; Petersson, G. A.; Ayala, P. Y.; Cui, Q.; Morokuma, K.; Malick, D. K.; Rabuck, A. D.; Raghavachari, K.; Foresman, J. B.; Cioslowski, J.; Ortiz, J. V.; Stefanov, B. B.; Liu, G.; Liashenko, A.; Piskorz, P.; Komaromi, I.; Gomperts, R.; Martin, R. L.; Fox, D. J.; Keith, T.; Al-Laham, M. A.; Peng, C. Y.; Nanayakkara, A.; Gonzalez, C.; Challacombe, M.; Gill, P. M. W.; Johnson, B. G.; Chen, W.; Wong, M. W.; Andres, J. L.; Head-Gordon, M.; Replogle, E. S.; Pople, J. A. *Gaussian 98*, revision B.02; Gaussian, Inc.: Pittsburgh, PA, 1998.

(21) *21.Cerius*^{2} *Polymer Builder, Operating Manual.*

(22) Scott, A. P.; Radom, L. Harmonic Vibrational Frequencies: An Evaluation of Hartree−Fock, Moller−Plesset, Quadratic Configuration Interaction, Density Functional Theory, and Semiempirical Scale Factors. *J. Phys. Chem.* **1996**, *100*, 16502−16513.

(23) Gaudreault, R. Mechanisms of Flocculation with Poly(ethylene oxide) and Novel Cofactors: Theory and Experiment. Ph.D. Thesis, Department of Chemistry, McGill University, Montreal, Canada, Dec 2003.

(24) Jochims, J. C.; Taigel, G.; Schmidt, O. Th. Protonenresonanz-Spektren und Konformationsbestimmung einiger natürlicher Gerbstoffe. *Liebigs Ann. Chem.* **1968**, *717*, 169−185.

(25) Yoshida, T.; Okuda, T. ^{13}C Nuclear Magnetic Resonance Spectra of Corilagin and Geraniin[1]. *Heterocycles* **1980**, *14* (11), 1743−1749.

(26) Wiliams, D. H.; Westwell, M. S. Aspects of Weak Interactions. *Chem. Soc. Rev.* **1998**, *27*, 57−63.

(27) Maclagan, R. G. A. R.; Malardier-Jugroot, C.; Whitehead, M. A.; Lever, M. Theoretical Studies of the Interaction of Water with Compensatory and Noncompensatory Solutes for Proteins. *J. Phys. Chem. A* **2004**, *108*, 2514−2519.

(28) Malardier-Jugroot, C.; Whitehead, M. A.; Maclagan, R. G. A. R.; Lever, M. An Explanation of the Denaturing of Proteins.

(29) *29. Kirk−Othmer Encyclopedia of Chemical Technology*, 4th ed.; Wiley: New York, 1998; Vol. 19, pp 701−722.

(30) Jeffry, G. A. *An Introduction to Hydrogen Bonding*; Oxford University Press: Oxford, 1997.

(31) Ochterski, J. W. *Thermochemistry in Gaussian 2000*; Gaussian, Inc.: **2000**, June 2, 1−19.

(32) Dunitz, J. D. Win Some, Lose Some: Enthalpy−Entropy Compensations in Weak Intermolecular Interactions. *Chem. Biol.* **1995**, *2*, 709−712.

(33) Steiner, T. The Hydrogen Bond in the Solid State. *Angew. Chem., Int. Ed.* **2002**, *41*, 48−76.

(34) Alkorta, I.; Elguero, J. Theoretical Study of Strong Hydrogen Bonds between Neutral Molecules: The Case of Amine Oxides and Phosphine Oxides as Hydrogen Bond Acceptors. *J. Phys. Chem. A* **1999**, *103*, 272−279.

(35) Hibbert, F.; Emsley, J. *Adv. Phys. Org. Chem.* **1990**, *26*, 269.

(36) Brion, C. E.; Cooper, G.; Zheng, Y.; Litvinyuk, I. V.; McCarthy, I. E. Imaging of Orbital Electron Densities By Electron Momentum Spectroscopy − A Chemical Interpretation on the Binary (e,2e) Reaction. *Chem. Phys.* **2001**, *270*, 13−30.

(37) Lee, J. C., Jr.; Peris, E.; Rheingold, A. L.; Crabtree, R. H. An Unsual Type of H···H Interactions: Ir−H···H−O and Ir−H···H−N Hydrogen Bonding and its Involvement in σ-Bond Metathesis. *J. Am. Chem. Soc.* **1994**, *116*, 11014−11019.

(38) Klooster, W. T.; Koetzle, T. F.; Siegbahn, P. E. M.; Richardson, T. B.; Crabtree, R. H. Study of the IN−H···H−B Dehydrogen Bond Including the Crystal Structure of BH_3NH_3 by Neutron Diffraction. *J. Am. Chem. Soc.* **1999**, *121* (27), 6337−6343.

(39) Pople, J. A.; Beveridge, D. L. *Approximate Molecular Orbital Theory*; McGraw-Hill: New York, 1970; p 43.

(40) Tretiak, S.; Mukamel, S. Density Matrix Analysis and Simulation of Electronic Excitations in Conjugated and Aggregated Molecules. *Chem. Rev.* **2002**, *102*, 3171−3212.

(41) Koch, U.; Popelier, P. L. A. Characterization of C−H−O Hydrogen Bonds on the Basis of the Charge Density. *J. Phys. Chem.* **1995**, *99*, 9747−9754.

(42) Gu, Y.; Kar, T.; Scheiner, S. Fundamental Properties of the CH−O Interaction: Is It a True Hydrogen Bond? *J. Am. Chem. Soc.* **1999**, *121*, 9411−9422.

(43) Scheiner, S. *Hydrogen Bonding. A Theoretical Perspective*; Oxford University Press: Oxford, 1997.

(44) Searle, M. S.; Westwell, M. S.; Williams, D. H. Application of a Generalised Enthalpy−Entropy Relationship to Binding Cooperativity and Weak Associations in Solution. *J. Chem. Soc., Perkin Trans. 2* **1995**, 141−151.

(45) Westwell, M. S.; Searle, M. S.; Klein, J.; Williams, D. H. Successful Predictions of the Residual Motion of Weakly Associated Species as a Function of the Bonding between Them. *Them. J. Phys. Chem.* **1996**, *100*, 16000−16001.

(46) Gaudreault, R.; Whitehead, M. A.; van de Ven, T. G. M. Mechanisms of flocculation with polyethyl oxide and novel cofactors. *Colloids Surf., A* **2005**, *268*, 131−146.

(47) Gaudreault, R.; van de Ven, T. G. M.; Whitehead, M. A. Theoretical study of the interactions of water with gallic acid and a PEO/TGG complex. *Molecular Simulation*, in press.